THE EFFECTS OF RAILPAD NONLINEARITY ON THE DYNAMIC BEHAVIOUR OF RAILWAY TRACKS

SG Koroma University of Nottingham, University Park, Nottingham, NG7 2RD, UK
MFM Hussein University of Nottingham, University Park, Nottingham, NG7 2RD, UK
JS Owen University of Nottingham, University Park, Nottingham, NG7 2RD, UK

1 INTRODUCTION

Railway tracks are commonly constructed with railpads that attenuate the level of vibration and impact transmitted to them from railway vehicles. The stiffness and damping properties of railpads have significant effects on track vibration and forces transmitted to the track substructure and underlying soil. When modelling track dynamic behaviour, it is most common to assume that these properties are linear and homogeneous. However, many studies, including Fenander (1997)[1], Thompson et al. (1998)[2], Maes et al. (2006)[3], etc., have shown that railpads exhibit pronounced nonlinear behaviour and their properties are dependent on preloads, among other factors like frequency and temperature. Characterising these dependencies is, to a large extent, subjective to a particular data set and is by no means a generic process. Therefore, this process should be carried out with the scope set to particular applications, for e.g. in railway track dynamics, the scope may be to predict the vibration levels in a track for which experimental data is available for the railpads.

The preload dependent behavior of a railway track with nonlinear railpads and ballast was studied by Wu and Thompson (1999)[4]. The preload dependent stiffnesses of the railpads were calculated using an equivalent continuous elastic foundation model. These were then used in a discretely supported track model in the frequency domain to obtain the track receptances and decay rates.

In this paper, a similar process is followed but the analysis is carried out in the time domain. In section 2, the stiffness and damping properties of the railpad are characterised for a studded rubber railpad that is commonly used on European railway tracks. Emperical expressions for the static and dynamic stiffnesses for a railpad are derived based on experimental data. A time domain based nonlinear Finite Element model is then developed in section 3 which incorporates the nonlinear railpads. The model consists of a rail that is discretely supported on railpads with preload dependent stiffness and damping under combined static and dynamic load to study the effects of nonlinearity on track dynamics. The model is solved in the time domain using a time integration scheme. Results are presented for the track dynamic response for various preload levels in section 4.

2 RAILPAD STIFFNESS AND DAMPING PROPERTIES

In this section, the static and dynamic load-displacement relationship of a railpad is presented. Based on experimental data presented in Thompson et al. (1998), empirical approximation is done for both the static and dynamic stiffnesses of a railpad using a Kelvin-Voigt visco-elastic model. This model consists of a spring and dashpot in parallel, with the spring representing the stiffness and the dashpot the damping properties of the railpad. Section 2.1 deals with the static stiffness whilst section 2.2 deals with the dynamic stiffness.

2.1 Static stiffness of railpads

Railpads have been found to exhibit strong nonlinear relationship between the applied static load and the corresponding displacement,[1,2]. In this section, the load-displacement relationship is characterised, and hence its static stiffness is described. Figure 1 shows a typical load-

displacement ($p-u$) curve and the associated stiffnesses that may result under the action of combined static and dynamic loading.

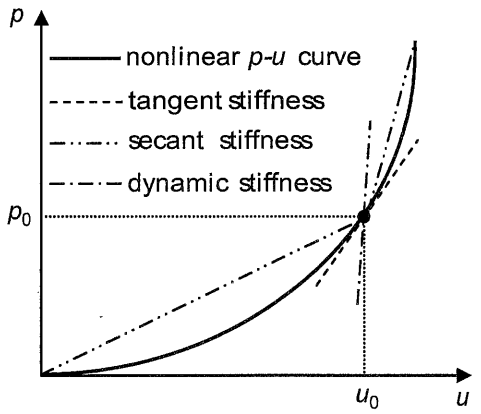

Figure 1: Static $p-u$ curve showing the tangent and secant stiffnesses at a given set of (p_0, u_0) and and an example of the dynamic stiffness when a dynamic load is superimposed on the preload

The force, p, on the railpad is a nonlinear function of the displacement, u, and can be described by a polynomial of degree α such that

$$p(u) = a_1 u + a_2 u^2 + \cdots + a_j u^j + \cdots + a_\alpha u^\alpha, \qquad \text{(Eq. 1)}$$

where $a_1, \ldots, a_\alpha$ are the coefficients and are obtained through the nonlinear curve fitting of experimental data, and j is a positive integer. In order to ensure that the fit between p and u is well conditioned, the approximation is done with p being in kN and u in mm. From Eq. 1 the secant stiffness, $k_s = \Delta p / \Delta u$, and the tangent stiffness, $k_t = dp/du$ can be obtained.

A seventh degree polynomial was found to sufficiently describe the $p-u$ relationship. The values of the polynomial coefficients obtained from the nonlinear curve fitting are: $a_1 = 20.00$ MN/m, $a_3 = 3.94$ MN/m^3, $a_5 = -1.78$ MN/m^5 and $a_7 = 3.28$ MN/m^7.The coefficients of the polynomial that are not included are zeros. Note that when fully unloaded, the railpad possesses an unloaded stiffness of a_1 MN/m.

In the construction of railway tracks, each railpad is preloaded by clips that hold it in place and by the weight of the rail that is supported within one fastener bay (i.e. 0.6 m length of rail). Wu and Thompson (1999)[4] calculated the total force to be about 20.36 kN, for 60E1 rail. To account for this initial preload, the reaction force in the railpad due to external track loads are added to this preload. However, it is assumed that the railpad is in static equilibrium at this preload, and all displacements are taken with reference to this point.

2.2 Dynamic stiffness of railpads

In addition to the preload dependence of the stiffness of a railpad, the stiffness is also dependent on frequency. Thompson et al (1998)[2] presented dynamic stiffness data for studded rubber railpads for five preload levels: 20, 30, 40, 60, and 80 kN, over a frequency range of 40-1000 Hz. Based on these data, approximations of the dynamic stiffness as a function of preload and frequency is derived using nonlinear curve fitting. A simple Kelvin-Voigt model is used here.

Consider the railpad is subjected to a combined preload, p_0, and a dynamic load $p_{dyn} = p_1 \exp(i\omega_0 t)$. The preload will induce a static displacement, u_0, resulting in a tangent stiffness, k_t at this configuration. It is assumed here that the dynamic load on the railpad is a linear function of the resulting dynamic displacement, u_{dyn}, i.e. neglecting any nonlinearity that may result from the dynamic load amplitude. The dynamic reaction force on the railpad is $k_t u_{dyn} + c\dot{u}_{dyn}$, c being the damping factor. The resulting dynamic stiffness is given by

$$k_{dyn} = k_t + i\omega_0 c . \qquad \text{(Eq. 2)}$$

Approximation of the railpad dynamic stiffness using Eq. 2 shows poor correlation with experimental data. However, better correlation is achieved when the theoretical dynamic stiffness is modified such that

$$\bar{k}_{dyn} = \gamma k_t + i\omega_0 c \qquad \text{(Eq. 3)}$$

where γ is a positive factor. The parameters required from the approximation are thus γ and c, since k_t can be calculated by differentiating Eq. 1. Values obtained for γ range from 3.2-3.6 for the five preload levels, giving an average value of 3.4. A constant value of 3.6 was used by Wu and Thompson (1999) for all frequency range. The damping factor follows the form

$$c = c_0(1+\beta^r) \qquad \text{(Eq. 4)}$$

where c_0 is the damping factor at a reference preload value p_c, $c_0 = 14.66 \times 10^3$ N.s/m, β is a ratio of the preload increment relative to p_c, i.e. $\beta = (p - p_c)/p_c$ and r is the exponential preload influence and has a value of 1.74. The reference preload is taken as the initial preload on the railpad due to the clips and mass of rail; i.e. p_c = 20.36 kN. Figure 2 shows a comparison of the experimental and fitted dynamic stiffness of the railpad. Good approximation can be seen to exist between the data and Eq. (Eq. 3).

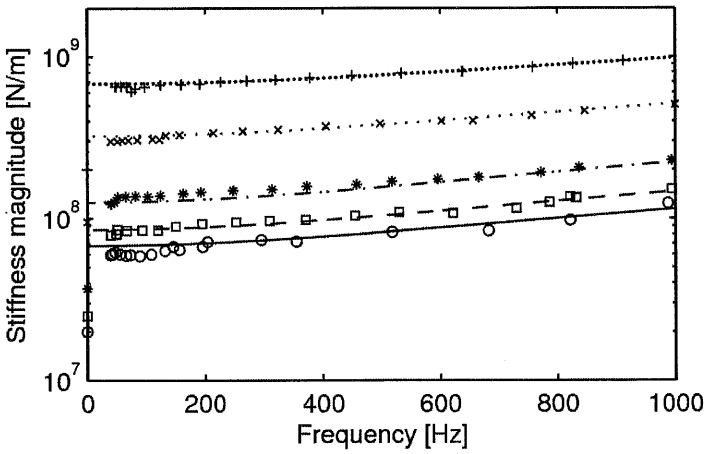

Figure 2: Approximations of railpad dynamic stiffness plotted against frequency for various preload levels (lines) compared with data points from [2] (markers). ——, o: 20; — — —, □: 30 ; — · —,*: 40; ····· , x: 60 and ·····, +: 80 kN;

One limitation of this Kelvin-Voigt model approximation is that the value constant value of γ for all $f > 0$ Hz exhibits a sudden change from a relatively low stiffness value to a much higher stiffness even though the dynamic contributions are small at low frequencies.

3 NONLINEAR FINITE ELEMENT TRACK MODEL

3.1 Model description

Figure 3 is a time domain Finite Elements (FE) based model of a railway track in which the rail is modelled as an Euler-Bernoulli beam with bending stiffness, EI, and mass per unit length, m. The rail is discretely supported on railpads at regular intervals, d, (typically 0.6 m) and is simply supported at the ends. For the purpose of studying only the effects of railpad properties on the dynamic behaviour of the track, it assumed that all track layers below the railpads are much stiffer than the railpads and can therefore be assumed to be rigid.

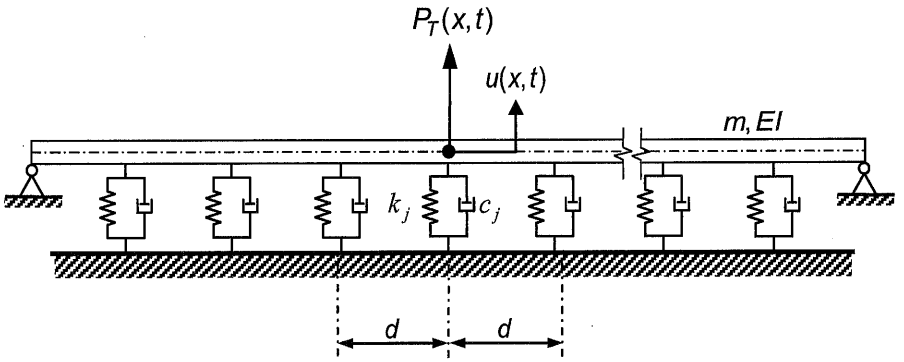

Figure 3: A model of a rail discretely supported on elastic foundation (railpad) and subjected to a non-moving combined static and dynamic load

The track is subjected to a stationary load, placed vertically at the midpoint of the beam, directly over a railpad, i.e. at $x = NL/2$. The load consists of a static component, P_0, and a dynamic component, $P(t)$. In order to investigate the dynamic behaviour of the track, $P(t)$ is defined as a harmonic function with amplitude, P_1, and angular frequency $\omega_0 = 2\pi f_0$, f_0 being the excitation frequency. Hence, the load on the track can be described by

$$P_T(x,t) = [P_0 + P_1 \exp(i\omega_0 t)]\delta(x - NL/2) \qquad \text{(Eq. 5)}$$

In the following sections, the discretisation of the rail, the system matrices and equation of motion of the track are presented.

3.2 Discretisation of the beam and system matrices

The rail is discretised into N finite elements of length, L, each having two nodes and four degrees-of-freedom (dofs), i.e. a vertical translation and rotation at each node. The length of each of these elements, L, is chosen such that $d/L = q$, where q is a positive integer. The track is composed of n railpad bays, hence the total number of elements in the track is $N = n \times q$. The resulting number of nodes is $N + 1$, number of dofs $N_D = 2(N + 1)$ and number of railpads of $N_D = n + 1$. The local stiffness and mass matrices for the ith beam element are given as

$$\mathbf{K}_{B,i} = \frac{EI}{L}\begin{bmatrix} 12/L^2 & 6/L & -12/L^2 & 6/L \\ & 4 & -6/L & 2 \\ & & 12/L^2 & -6/L \\ Sym & & & 4 \end{bmatrix}, \mathbf{M}_i = \frac{mL}{420}\begin{bmatrix} 156 & 22L & 54 & -13L \\ & 4L^2 & 13L & -3L \\ & & 156 & -22L \\ Sym & & & 4L^2 \end{bmatrix}. \qquad \text{(Eq. 6)}$$

The local displacement and force vectors of the ith element are respectively given by

$$\mathbf{u}_i = \{u_{2i-1}, u_{2i}, u_{2i+1}, u_{2i+2}\}^T \text{ and } \mathbf{P}_i = \{P_{2i-1}, P_{2i}, P_{2i+1}, P_{2i+2}\}^T . \quad \text{(Eq. 7)}$$

Global system matrices and vectors must be formed to describe the dynamic behavior of the track as a whole. This is considered in the next section.

3.3 Assembly of global track matrices and equation of motion

The global stiffness and mass matrices of the beam structure are assembled using compatibility conditions at the nodes, i.e. displacement, slope and bending moments are continuous. In this way, the local matrix components corresponding to the mutual nodes between two successive elements are overlapped. The assembly of the global matrices can be summarised in the following equations:

$$\mathbf{M} = \sum_{i=1}^{N} \tilde{\mathbf{M}}_{\{2i-1:2i+2,2i-1:2i+2\}} + \mathbf{M}_i ; \text{ and } \mathbf{K}_B = \sum_{i=1}^{N} \tilde{\mathbf{K}}_{\{2i-1:2i+2,2i-1:2i+2\}} + \mathbf{K}_{B,i} ; \quad \text{(Eq. 8)}$$

where $\tilde{\mathbf{M}}$ and $\tilde{\mathbf{K}}$ are $N_D \times N_D$ null matrices for the stiffness and mass of the beam respectively.
In addition to the global mass and stiffness matrices for the beam, global stiffness and damping matrices of the railpads are formed as follows

$$\mathbf{C} = \sum_{i=1}^{N_R} \tilde{\mathbf{C}}_{\{2q(j-1)+1,2q(j-1)+1\}} + c_j ; \text{ and } \mathbf{K}_P = \sum_{i=1}^{N_R} \tilde{\mathbf{K}}_{\{2q(j-1)+1,2q(j-1)+1\}} + k_j ; \quad \text{(Eq. 9)}$$

where $\tilde{\mathbf{C}}$ is an $N_D \times N_D$ null matrix for the damping of the railpad, c_j and k_j are the preload dependent stiffness and damping. The total track stiffness matrix is thus $\mathbf{K} = \mathbf{K}_B + \mathbf{K}_P$.
The differential equation of motion can now be written for the whole track structure. The differential equation of motion of a beam supported on a Kelvin-Voigt foundation is given by

$$\mathbf{M}\ddot{\mathbf{u}} + \mathbf{C}\dot{\mathbf{u}} + \mathbf{K}\mathbf{u} = \mathbf{P}, \quad \text{(Eq. 10)}$$

Where $\mathbf{u}$ and $\mathbf{P}$ are the global nodal displacement and external force vector, $\mathbf{P}$ consists of only one non-zero entry being $P_T(x,t)$.

3.4 Solution of equation of motion

The procedure for solving the differential equations of motion in Eq. 10 requires that the preloaded stiffnesses of the railpads be calculated based on the static load-displacement relationship and according to the magnitude of the static load. These are then used as input to study the dynamic behaviour of the track.

3.4.1 Calculation of preloaded stiffnesses

To obtain the preloaded stiffnesses of the railpads under the effect of the static load, the following nonlinear static equation needs to be solved

$$\mathbf{F}(\mathbf{u}_0) = \mathbf{P}_0 \quad \text{(Eq. 11)}$$

Where $\mathbf{F}(\mathbf{u}_0)$ is the nonlinear reaction force vector; $\mathbf{F}(\mathbf{u}_0) = \mathbf{K}(\mathbf{u}_0)\mathbf{u}_0$, with $\mathbf{K}(\mathbf{u}_0)$ being the nonlinear static stiffness as a function of the static displacements, $\mathbf{u}_0$, $\mathbf{P}_0$ is the external nodal force vector consisting of P_0 as the only non-zero element, at the corresponding dof where the external load is applied.
A simple Newton-Raphson iteration procedure is adopted to obtain the static displacements of the pads, and hence the preloaded stiffnesses. This procedure is summarised as

$$\mathbf{K}^{(i-1)}\Delta\mathbf{u}_0^{(i)} = \mathbf{P}_0 - \mathbf{F}^{(i-1)}$$
$$\mathbf{u}_0^{(i)} = \mathbf{u}_0^{(i-1)} + \Delta\mathbf{u}_0^{(i)} \qquad \text{(Eq. 12)}$$

where $\mathbf{K}^{(i-1)}$ is the consistent tangent stiffness matrix at the configuration corresponding to the static displacement $\mathbf{u}_0^{(i-1)}$, for 'i' being the number of iterations. Convergence of Eq. 12 is achieved by satisfying a predefined convergence criterion that guarantees the degree of accuracy required for the solution. Once the static displacements of the pads have been obtained, the preloaded pad stiffnesses corresponding to these displacements are then computed.

3.4.2 Solution for the dynamic response of the track

The solution for the dynamic response of the track is carried out using the composite implicit time integration procedure presented by Bathe and Irfan-Baig (2005)[5]. The general stability of this scheme has been thoroughly discussed therein.

Results are now presented in section 4 to study the effect the preload dependence of the railpad on the dynamic behaviour of the track.

4 RESULTS AND DISCUSSIONS

The parameter used for the numerical simulations are: 60E1 rail with mass and bending stiffness of m = 60.21 kg/m, EI = 6.4 MN.m^2, railpad spacing, d = 0.6 m and the length of each element L = 0.3 m. The railpad properties are as described in section 2.

4.1 Results for preloads and preloaded stiffnesses

Tables 1 and 2 contain respectively the static preloads and stiffnesses for the case when a static load is positioned directly over the railpad at the middle of the track. Due to symmetry, only the pads on the positive side of the load have been presented.

Table 1: Preloads (in kN) on the railpads in the vicinity of the static load

Pad position	Static Load (kN)				
from load (m)	0	25	50	75	100
0	20.36	28.47	37.26	48.24	62.57
0.6	20.36	26.26	32.09	37.41	41.75
1.2	20.36	23.08	25.56	27.50	28.73
1.8	20.36	21.04	21.62	22.03	22.24
2.4	20.36	20.18	20.00	19.83	19.69
3.0	20.36	20.02	19.70	19.45	19.28
∞	initial preload of 20.36 kN				

The preload values given in Table 1 compare with values given Wu and Thompson (1999) to within 10%, with the differences being accounted for by the absence of a ballast layer in the current model and the approximation of the nonlinear fit to the load-deflection relationship of the railpad. It can be seen from Tables 1 and 2 that when there is no external load on the track, all preloads and stiffnesses of the railpads are equal to the unloaded values of 20.36 kN and 20 MN/m respectively. They then increase for higher levels of preload, but beyond a distance of about 3 m from the load, the pads are almost insensitive to load and remain fairly unloaded.

Table 2: Preloaded stiffnesses (in MN/m) of the railpads in the vicinity of the static load

Pad position from load (m)	Static Load (kN)				
	0	25	50	75	100
0	20.00	21.74	28.60	53.56	102.16
0.6	20.00	20.96	23.60	28.80	36.53
1.2	20.00	20.21	20.75	21.37	21.85
1.8	20.00	20.01	20.05	20.08	20.10
2.4	20.00	20.00	20.00	20.01	20.01
3.0	20.00	20.00	20.00	20.00	20.00
∞	unloaded stiffness of 20 MN/m				

Results are now presented for the dynamic response of the track. Validation of the FE model is first carried out in section 4.2 and the effect of preload is studied in section 4.3.

4.2 Validation of the FE model

Results are first presented to compare the nonlinear FE model with the solution of the beam on elastic foundation using the Fourier Transformation Method (FTM). The comparison is done for the case of $P_0 = 0$ and a harmonic load with unit amplitude (i.e. $P_1 = 1$ N). At this configuration, the stiffness corresponds to the linear value. Figure 4 shows the peak steady-state displacement amplitude and phase angle for a point on the beam directly under the load, plotted against the excitation frequency of the load.

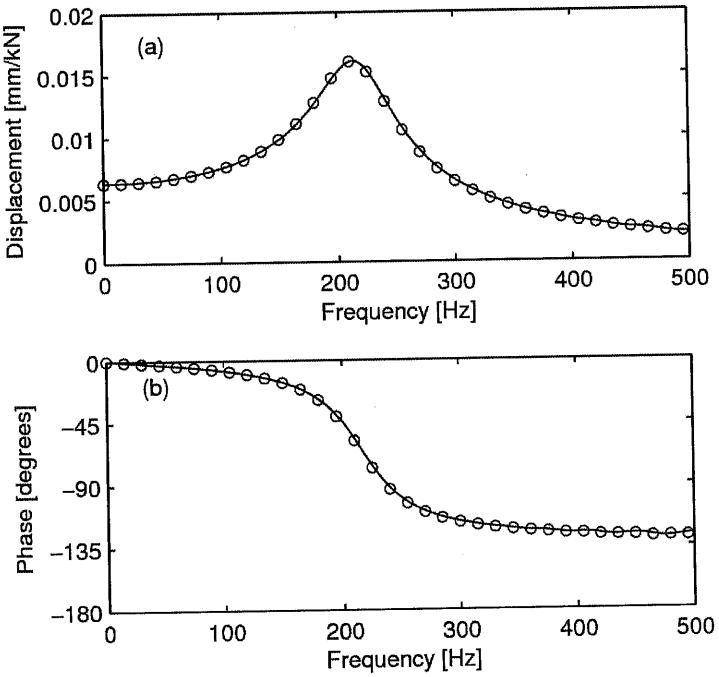

Figure 4: (a) Peak steady-state displacement amplitude and (b) phase angle for a point directly under the load plotted against excitation frequency of the oscillating load. ——: FEM, o: FTM.

It is apparent that the results are in good agreement over the range of frequencies shown, with the response amplitudes increasing with increase in frequency up until the cut-on frequency, $f_{co} \approx 1/2\pi\sqrt{\gamma a_1 / md} = 218$ Hz, before gradually decaying beyond this point. This occurs since the beam vibrates in phase with the load up to the cut-on frequency, but out of phase beyond this point.

4.3 Effect of the magnitude of the static load

Results are now presented for the nonlinear FE model. Five levels of static load are considered; 0, 25, 50, 75 and 100 kN. Superimposed on each of these is a unit amplitude dynamic load. The preloaded stiffness distribution is calculated using Eq. 12 and then used as input to study the dynamic response. Figure 5 shows the dynamic displacement amplitude and phase as a function of excitation frequency for a point that is directly under the load.

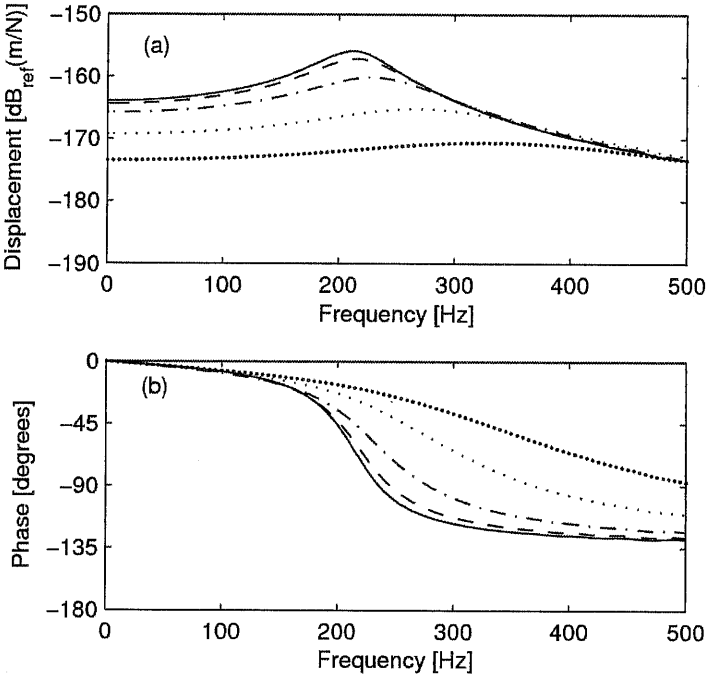

Figure 5: (a) Peak steady-state displacement amplitude and (b) phase angle for a point directly under the load plotted against frequency of the oscillating load for five preload levels. ——: 20; – – –: 30; —• —: 40; ..... : 60 and •••••••••: 80 kN.

The general trend is that the dynamic response amplitudes and phase angles reduce with increase in preload due to the increased preloaded stiffness of the pads in the vicinity of the load. This in turn leads to an increased cut on frequency. For the range of preload shown, the peak response amplitudes vary by almost 15 dB between the linear stiffness case at 0 kN and the strongly nonlinear case at 100 kN.

Such a large difference between the loaded and unloaded behavior suggests that the preload effect should be accounted since the constant stiffness model largely overestimates the track response.

5 REFERENCES

1. A. Fenander., 'Frequency dependent stiffness and damping of railpads', Proceedings of the Institution of Mechanical Engineers, 211(Part F), 51-62. (1997).
2. D.J. Thompson, W.J. van Vliet and J.W. Verheij., 'Development of an indirect method for measuring the high frequency dynamic stiffness of resilient elements', Journal of Sound and Vibration, 213(1), 169-188. (1998).
3. J. Maes, H. Sol and P. Guillaume., 'Measurements of the dynamic railpad properties', Journal of Sound and Vibration, 293, 557-565. (2006).
4. T.X. Wu and D.J. Thompson., 'The effects of local preload on the foundation stiffness and vertical vibration of railway track', Journal of Sound and Vibration, 219(5), 881-904. (1999).
5. K.-J. Bathe and M.M. Irfan-Baig., 'On a composite implicit time integration procedure for nonlinear dynamics', Computers and Structures, 83, 2513-2524. (2005).